Hindawi Publishing Corporation
Advances in Acoustics and Vibration
Volume 2010, Article ID 174361, 6 pages
doi:10.1155/2010/174361

Research Article

A Consistency Test of Thickness and Loading Noise Codes Using Ffowcs Williams and Hawkings Equation

Sofiane Khelladi and Farid Bakir

DynFluid Laboratory, Arts et Métiers ParisTech, 151, boulevard de l'Hôpital, 75013 Paris, France

Correspondence should be addressed to Sofiane Khelladi, sofiane.khelladi@paris.ensam.fr

Received 12 March 2010; Accepted 19 May 2010

Academic Editor: Kim M. Liew

The thickness noise predicted by the Ffowcs Williams and Hawkings (FW&H) equation depends on the normal velocity v_n which is very sensitive to the meshing size. Isom showed that in far field a monopolar source is equivalent to a dipolar source induced by a uniform distribution of the load on the entire moving surface. The main objective of this paper is to determine a specific expression of Isom's thickness noise in time and frequency domains for subsonic fans. The scope of the proposed expression of Isom's thickness noise is to define a benchmark test of consistency for thickness and loading noise codes in both time and frequency domains for subsonic fans when using the free field solution of FW&H's equation.

1. Introduction

In free field, Isom showed in [1] that the acoustic pressure generated by a mopole is equivalent to these generated by dipole induced by a uniform load equal to $\rho_0 c^2$ over a moving surface. Consequently, the calculation of the thickness noise becomes completely independent of the normal velocity v_n over the surface.

Farassat shows in [2, 3] that it is more suitable to determine the thickness noise using Isom's formulation than methods based on the resolution of Ffowcs Williams and Hawkings (FW&H) equation [4] using fluctuating velocity. The latter presents an important variation on the surface which makes the numerical integration very sensitive to the meshing resolution. On the other hand, Isom's thickness noise formula can present some difficulties for rotating machinery because of its sensitivity to the geometry of the blade tips [5].

Isom's thickness noise formula was used by Ghorbaniasl and Hirsch [6] as a consistency benchmark to show that it should not exist discrepancy between FW&H's thickness noise and Isom's noise when Farassat 1A formulation presented by Farassat and Succi in [7] is numerically solved in time domain. Khelladi et al. presented in [8] a specific formulas of thickness noise in time and frequency domains for subsonic fans based on initial Isom's formulation.

In this paper, we will present a validation of the formulas proposed in [8]. In Section 2 a brief remainder of the Isom's thickness noise formulas is presented. To illustrate the potential of the proposed approach, two examples are discussed in Section 3 to review a code using FW&H equation. In example 1, a two-bladed rotor will be studied. The effect of each part of the thickness noise as well as the effect of the tip Mach number on the overall noise will be shown. In example 2, thickness noise obtained by the FW&H equation for a high-rotational speed centrifugal fan [9] will be compared to that obtained by the proposed formulas. The method is used as a consistency test in time and frequency domains for the two examples. Finally, conclusions are drawn in Section 4.

2. Isom's Thickness Noise

Let $f(\mathbf{x}, t) = 0$ be a function taking into account the geometry and the kinematics of a moving body surface, defined such as $f > 0$ outside the body, see Figure 1. Let $H(f)$ be the Heaviside function.

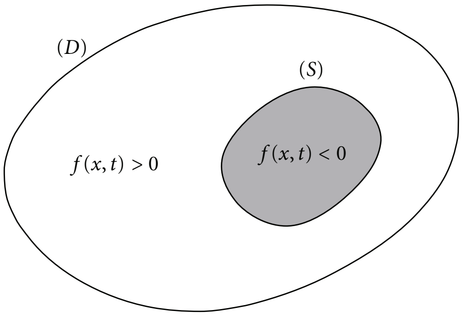

Figure 1: Calculation domain.

According to [3], the wave equation corresponding to the trivial function $\rho_0 c^2[1-H(f)]$ is given by

$$\left[\frac{1}{c^2}\frac{\partial^2}{\partial t^2} - \nabla^2\right]\{\rho_0 c^2[1-H(f)]\} = \frac{\partial}{\partial t}[\rho_0 v_n \delta(f)] + \frac{\partial}{\partial x_i}[\rho_0 c^2 n_i \delta(f)], \tag{1}$$

where $n_i = \partial f/\partial x_i$ and $v_n = \mathbf{v}\cdot\mathbf{n}$ are, respectively, the local unit normal vector and the local normal velocity on the body surface.

2.1. Time Domain Solution. The far and free field solution of (1) is given by

$$\rho_0 c^2[1-H(f)] = -\frac{1}{4\pi}\frac{\partial}{\partial t}\int_S \left[\frac{\rho_0 v_n}{rD}\right]_{\text{ret}} dS + \frac{1}{4\pi}\frac{\partial}{\partial x_i}\int_S \left[\frac{\rho_0 c^2 n_i}{rD}\right]_{\text{ret}} dS, \tag{2}$$

where $D = |1 - M_r|$ is the Doppler factor.

Outside the body $H(f) = 1$, then,

$$\rho_0 c^2[1-H(f)] = 0. \tag{3}$$

Equation (2) gives then,

$$\frac{1}{4\pi}\frac{\partial}{\partial t}\int_S \left[\frac{\rho_0 v_n}{rD}\right]_{\text{ret}} dS = \frac{1}{4\pi}\frac{\partial}{\partial x_i}\int_S \left[\frac{\rho_0 c^2 n_i}{rD}\right]_{\text{ret}} dS. \tag{4}$$

This equality shows that the monopole source solution is not unique. It is, also, equal to a dipole source induced by a steady and uniform load $\rho_0 c^2$ over the moving body surface.

Isom's thickness noise is then given by

$$p'_{\text{Isom}}(\mathbf{x},t) = \frac{1}{4\pi}\frac{\partial}{\partial x_i}\int_S \left[\frac{\rho_0 c^2 n_i}{rD}\right]_{\text{ret}} dS. \tag{5}$$

In far field on can show that

$$p'_{\text{Isom}}(\mathbf{x},t) = -\frac{1}{4\pi}\int_S \left[\frac{\mathbf{r}}{cDr}\left\{\frac{1}{r}\frac{\partial}{\partial \tau}\left(\frac{\mathbf{F}}{D}\right) + \frac{\mathbf{F}}{r^3 D}c\mathbf{r}\cdot\mathbf{M}\right\}\right]_{\text{ret}} dS, \tag{6}$$

where $t = \tau + r/c_0$ is the reception time and $\mathbf{F} = \rho_0 c^2 \mathbf{n}$ is the force induced by the uniform load $\rho_0 c^2$.

In far field, the term in $1/r^3$ is neglected, (6) becomes after expansion

$$p'_{\text{Isom}}(\mathbf{x},t) = \frac{1}{4\pi}\int_S \left[\underbrace{\frac{\mathbf{r}\cdot\mathbf{F}}{cD^3 r^2}\frac{\partial D}{\partial \tau}}_{\text{I}} - \underbrace{\frac{\mathbf{r}\cdot(\partial \mathbf{F}/\partial \tau)}{cD^2 r^2}}_{\text{II}}\right]_{\text{ret}} dS. \tag{7}$$

D is given as function of r, by: $D = |1 + (1/c)(\partial r/\partial \tau)|$.

Part (I) of (7) expresses the unsteadiness of the source motion while part (II) expresses the effect of the rotating load ($\rho_0 c^2$) source.

Equation (7) can, then, be written as

$$p'_{\text{Isom}}(\mathbf{x},t) = p'_{\text{I}}(\mathbf{x},t) + p'_{\text{II}}(\mathbf{x},t), \tag{8}$$

where

$$\begin{aligned} p'_{\text{I}}(\mathbf{x},t) &= \frac{1}{4\pi}\int_S \left[\frac{\mathbf{r}\cdot\mathbf{F}}{c^2 r^2 |1 + (1/c)(\partial r/\partial \tau)|^3}\frac{\partial^2 r}{\partial \tau^2}\right]_{\text{ret}} dS, \\ p'_{\text{II}}(\mathbf{x},t) &= -\frac{1}{4\pi}\int_S \left[\frac{\mathbf{r}\cdot(\partial \mathbf{F}/\partial \tau)}{cr^2 |1 + (1/c)(\partial r/\partial \tau)|^2}\right]_{\text{ret}} dS. \end{aligned} \tag{9}$$

Equations (9) are nothing more than the loading noise parts of Formulation 1A of Farassat. As it is written, because of the existence of partial derivatives in the denominators, the formulas are ambiguous to interpretation. This ambiguity is a mathematical subtlety discussed in the NASA publication of Farassat [10]. In our case, this form of writing will be very useful for the continuation of the development and the ambiguity will be circumvented. An exact expression of r will be given below and partial derivatives will be fully defined.

2.2. Isom's Thickness Noise for Fans. Let us consider a fan turning at a velocity Ω. The angular position of a point on the blade is related to the moment of noise emission τ by $\Psi = \Omega\tau + \Psi_0$ where Ψ_0 is the initial position at $\tau = 0$. Suppose that $\Psi_0 = 0$ at $\tau = 0$. On Figure 2, S is a noise source rotating around e_3 with an angular velocity Ω and a distance r_s. $\mathbf{F}$, a force applied by the fluid on the surface on S, defined by its radial, tangential, and axial components (F_r, F_t, F_a). O is an observer defined by (r_0, φ, θ) and $\mathbf{r}$ the distance between S and O.

In paper [8] Khelladi et al. demonstrated that the two parts of the thickness noise for fans can be given by

$$p'_{\text{I}}(\mathbf{x},t) = \frac{\Omega^2 \sin(\theta)}{4\pi r_0 c^2} \times \int_S \frac{r_s \cos(\Omega\tau - \varphi)\{\mathfrak{A}\}}{|1 + A\sin(\Omega\tau - \varphi)|^3} dS, \tag{10}$$

where $\mathfrak{A}$ denotes $\sin(\theta)\cos(\Omega\tau - \varphi)F_r + \sin(\theta)\sin(\Omega\tau - \varphi)F_t + \cos(\theta)F_a$.

$$p'_{\text{II}}(\mathbf{x},t) = \frac{\Omega\sin(\theta)}{4\pi r_0 c}\int_S \frac{\sin(\Omega\tau - \varphi)F_r + \cos(\Omega\tau + \varphi)F_t}{|1 + A\sin(\Omega\tau - \varphi)|^2} dS, \tag{11}$$

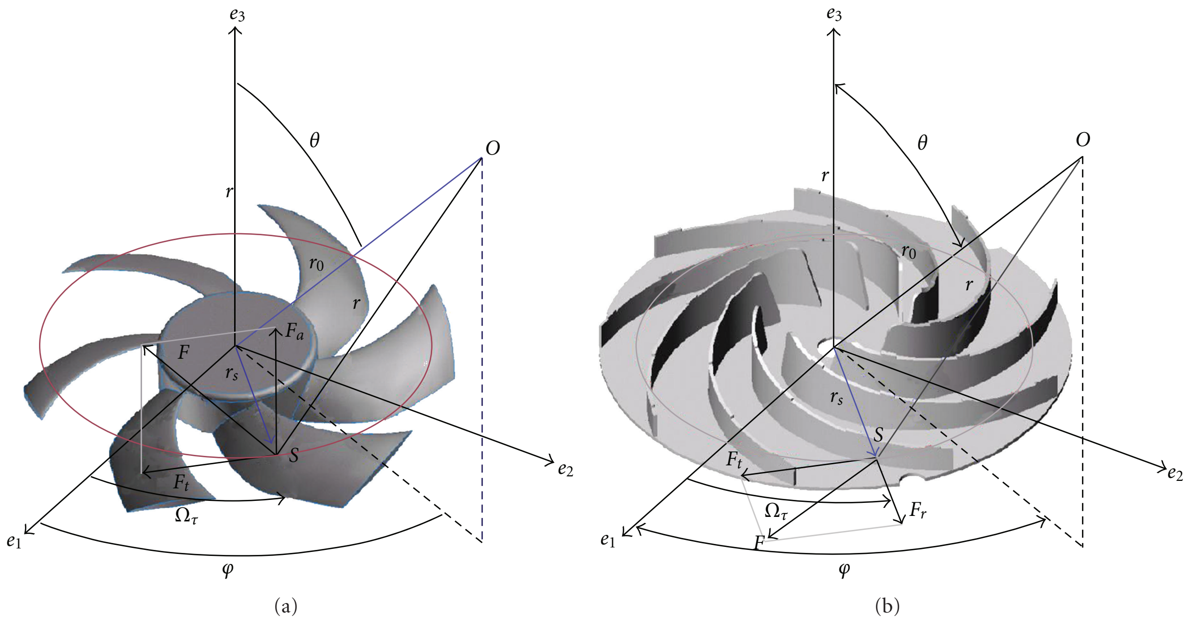

FIGURE 2: Reference frame: (a) Axial fan ($F_r = 0, F_t, F_a$), (b) Centrifugal fan ($F_r, F_t, F_a = 0$).

where $A = (r_s\Omega/c)\sin(\theta)$.

If $\mathbf{n}$ is local unit normal vector on the blade surface in the moving reference frame, then, the force three components are given by $F_r = \rho_0 c^2(\mathbf{n} \cdot \mathbf{n}_r)$, $F_t = \rho_0 c^2(\mathbf{n} \cdot \mathbf{n}_t)$, and $F_a = \rho_0 c^2(\mathbf{n} \cdot \mathbf{n}_a)$, where $\mathbf{n}_r$, $\mathbf{n}_t$ and $\mathbf{n}_a$ are, respectively, the local unit vectors in radial, tangential, and axial directions.

The direction of $\mathbf{F}$ components depends on the direction of the source rotation and position.

It is noticed that the axial component F_a of the load $\rho_0 c^2 n_i$ does not exist in (11). So, for centrifugal fans, part (II) of thickness noise is influenced by both radial and tangential components of the load $\rho_0 c^2\mathbf{n}$, whereas, for axial fans, only tangential component has influence on it.

Let us consider a Z blades fan, the overall acoustic pressure generated by the fan is given by

$$P'_{\text{Isom}}(\mathbf{x}, t) = \sum_{n=1}^{Z} p'_{\text{Isom}}\left(\mathbf{x}, t + \frac{\alpha_n}{\Omega}\right), \tag{12}$$

where p' is the acoustic pressure of one blade and α_n is the angle between two successive blades.

2.3. Frequency Domain Solution. In frequency domain it was demonstrated in [8] that the two components of the thickness for a Z-blades fan are given by

$$P'^{(m)}_{\text{I}}(\mathbf{x}) = \frac{Z\Omega^2\sin(\theta)}{8\pi^2c^2r_0}e^{imZ(\Omega(r_0/c)+\varphi)} \times \int_S\int_{-\varphi}^{2\pi-\varphi}\frac{r_s\cos(\xi)\{\mathfrak{X}\}}{(1+A\sin(\xi))^2}e^{imZ(\xi-A\cos(\xi))}d\xi dS,$$

$$P'^{(m)}_{\text{II}}(\mathbf{x}) = \frac{Z\Omega\sin(\theta)}{8\pi^2cr_0}e^{imZ(\Omega(r_0/c)+\varphi)} \times \int_S\int_{-\varphi}^{2\pi-\varphi}\frac{\sin(\xi)F_r+\cos(\xi+2\varphi)F_t}{|1+A\sin(\xi)|}e^{imZ(\xi-A\cos(\xi))}d\xi dS, \tag{13}$$

where $\mathfrak{X}$ denotes $\sin(\theta)\cos(\xi)F_r + \sin(\theta)\sin(\xi)F_t + \cos(\theta)F_a$ and $\xi = \Omega\tau - \varphi$ and $A = (r_s\Omega/c)\sin(\theta)$.

Contrary to (10) and (11), (13) needs a surface integral over only one blade, which constitute a consequent time and numerical storage reduction.

Hawkings and Lowson showed in [11] that for high-Mach numbers and high-sound levels, the effects of nonlinear acoustic propagation must be taken into account. They stated that nonlinear propagation causes some noticeable changes in the observed acoustic field, especially in its spectral characteristics. Consequently, the formulas described above in frequency domain will be more appropriate for low-Mach numbers and linear acoustic propagation cases.

3. Examples and Discussion

3.1. Example 1: A Two-Bladed Rotor. A NACA 0010 two-bladed rotor at several tip Mach numbers in time domain is studied in this example. The blades are 5 m in outer radius and 1 m in inner radius with a constant chord of 0.4 m and 10% of thickness ratio along the entire span of the blade. The observer is in the rotor plane and 50 m from the center. The surface expressed by $f(\mathbf{x}, t) = 0$ is assumed to be the upper, the lower, and the tip surfaces of the blade.

Figure 3 shows the acoustic pressure given by (12) for 0.2, 0.5, and 0.9 tip Mach numbers. To review the effect

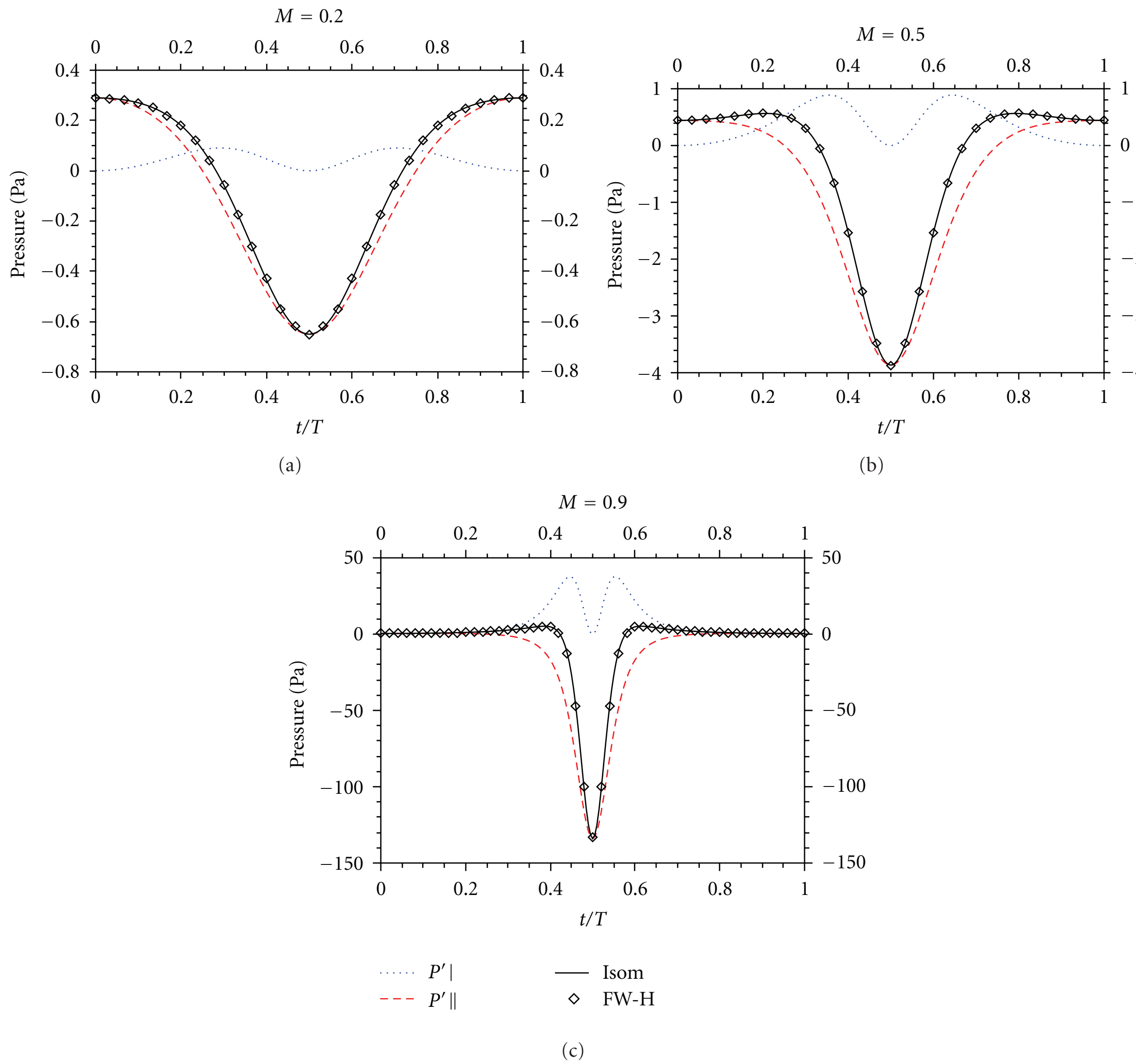

Figure 3: Acoustic pressure signal: (a) Tip Mach number 0.2, (b) Tip Mach number 0.5, (c) Tip Mach number 0.9.

of each part of the acoustic pressure, expressions given by (10) and (11) in time domain are also included in this figure. Recall that p'_{I} given by (10) expresses the effect of the kinematics and the geometry of the source and p'_{II} given by (11) expresses the effect of the moving load $\rho_0 c^2$.

For low-tip Mach number (Figure 3(a)), the amplitude of p'_{I} is very small compared to p'_{II} and the overall acoustic pressure p'_{Isom} results mainly from the effect of the moving load $\rho_0 c^2$. When the tip Mach number increases (Figures 3(b) and 3(c)), the effect of the kinematics and the geometry of the source become more important on the overall acoustic pressure p'_{Isom}. If we compare now the acoustic pressure obtained by Isom and by FW&H, we observe a good agreement between the two formulation. That means that the numerical implementation is correct and the meshing of tip and root surfaces of the blade was correctly performed. For more details, an assessment of the causes of errors on the time-based formulation is discussed in [12] in which the same example was treated but using a decreasing thickness ratio at the extremities of the blade. The influence of the tip surfaces grid refinement can be found in [6].

3.2. Example 2: A High Rotational Velocity Centrifugal Fan. Centrifugal fans, made up of an impeller, a diffuser and a return channel (Figure 4), are widely used in vacuum cleaners. These fans turn at a relatively high rotational speeds of about 35000 rpm. Their low efficiency of about 30% and their high acoustic levels are mainly due to the flow disorganization in the impeller-diffuser interface, the junction diffuser-return channel, and the exit of the return channel [9, 13]. The unsteady flow is strong and can reache 250 m/s. The aerodynamic and geometrical characteristics at the operating point are given, respectively, in Tables 1 and 2.

In [9], Khelladi et al. showed that the thickness noise of this centrifugal fan calculated by the Ffowcs Willams and Hawkings equation is not negligible compared to the dipole

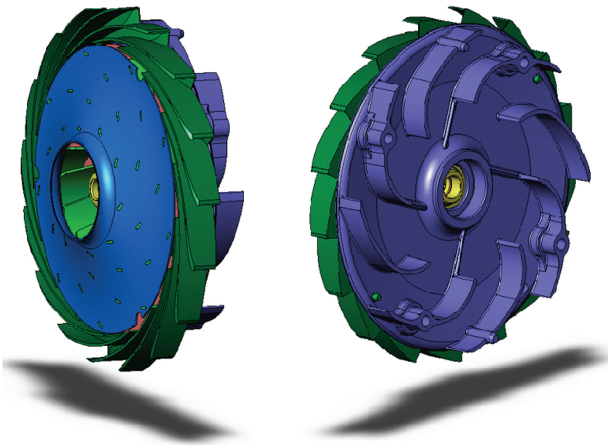

Figure 4: Centrifugal fan: Impeller, diffuser, and return channel.

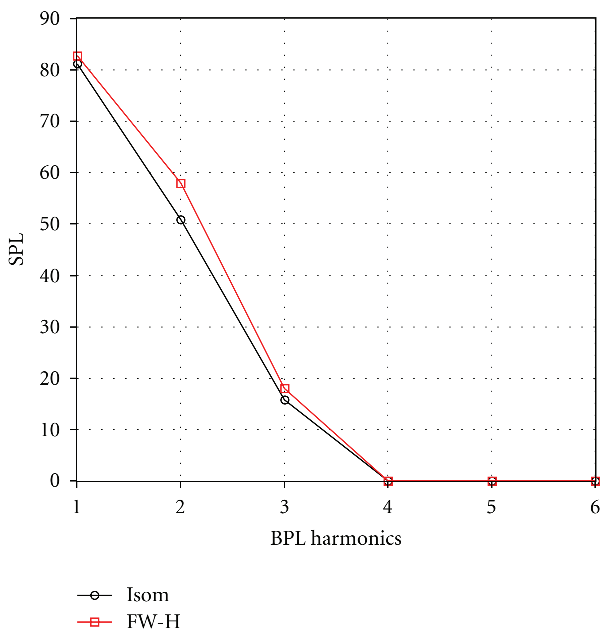

Figure 5: SPL versus blade passing frequency harmonics ($M = 0.56$) at 1 m from the source.

source. It was also shown that the corresponding acoustic pressure in frequency domain is given by

$$p'^{(m)}_{\text{thickness}}(\vec{x}) = \frac{imZ^2\Omega\rho_0}{4\pi r_0} e^{imZ\Omega(r_0/c)} \times \iint_S \sum_{k=-\infty}^{+\infty} e^{i(mZ-k)(\varphi-\pi/2)} J_{mZ-k}(A) v_n^{(k)} dS, \tag{14}$$

where

$A = mZ\Omega(r_s/c_0)\sin(\theta)$ and $M_{rs} = r_s\Omega/c_0$

$J_{mZ-k}(A)$: first kind Bessel function.

For both FW&H and Isom thickness noise formulations, the observer is placed in the rotor plane and 1 m from the center. The surface expressed by $f(\mathbf{x}, t) = 0$ is assumed to be the pressure and the suction sides of the impeller blade.

Table 1: Aerodynamic characteristics at operating point.

Description	Value
Head	1 300 (m)
Flow rate	35×10^{-3}(m^3/s)
Rotational speed	34 560 (rpm)
Specific speed	29

Table 2: Geometrical characteristics of the centrifugal fan.

Description	Impeller	Diffuser	Return channel
Radius of blade inlet (mm)	18	52.7	60
Span of the blade at the entry (mm)	13	6.48	11
Inlet blade angle (°)	64	85	74
Inclination Angle of the blade inlet (°)	85.8	0	0
Radius of blade exit (mm)	52	66.1	33
Span of the blade at the exit (mm)	5.4	8.43	12
Angle of blade exit (°)	64	71.6	15
Inclination angle of the blade exit (°)	0	0	0
Blade number	9	17	8
Blade thickness (mm)	0.8	0.9	1.6

Figure 5 presents the spectra of the thickness noise given by both FW&H and Isom equations as a function of harmonics of the Blade Passing Frequency (BPF).

It was observed that the calculation of the Isom's thickness noise is very sensitive to the numerical integration model mainly for frequencies corresponding to high harmonics. For the three first harmonics the variation of the SPL between FW&H and Isom is about 2% for harmonic 1 and about 14% for harmonics 2 and 3. This large variation is probably caused by the absence of the effect of the other parts of the fan in Isom's modeling. For this case, only harmonic 1 calculated by the FW&H equation can be validated by Isom. The overall acoustic level (OASPL) is dominated by the first harmonic: 81.20 dB given by Isom and 82.81 dB given by FW&H (a variation of about 2%). The proposed Isom's formulas give then a good estimation of the OASPL.

4. Conclusion

In this paper, specific formulas of thickness noise in time and frequency domains for subsonic fans based on the initial Isom's formulation were defined and used as a benchmark test of consistency when using the free-field solution of the FW&H's equation. The proposed formulas highlight also the effect of each geometrical parameter of the fan on the overall thickness noise and present a fast computational mean and low memory storage capability since the acoustic pressure in frequency domain is calculated for only one blade. The overall acoustic pressure was decomposed into two parts; the first one highlighted the effect of the kinematics and the geometry of blades, and the second one highlighted the effect of the moving load over blades expressed by $\rho_0 c^2$.

To illustrate the use of the proposed formulas, two examples were treated. The first one concerns a two-bladed rotor at several tip Mach numbers. Thickness noise was calculated using Isom's and FW&H's formulations. Concerning Isom's formulation, the results showed a different effect of the two parts of the acoustic pressure, depending on whether we used low or high Mach number. A good agreement between Isom's and FW&H's formulations was observed. That proves that the numerical implementation was correctly set up, and the meshing of tip and root surfaces of the blade was correctly performed.

The second example concerns a high rotational speed centrifugal fan. For this case, the thickness noise was calculated by the FW&H equation and compared to the proposed formulas at frequency domain. The result showed that only harmonic 1 calculated by the FW&H equation was correctly estimated by Isom. It was observed also as a good estimation of the overall SPL (only 2% of variation). For this case, one can conclude that the proposed consistency test is at least applicable to validate the first harmonic SPL and the overall SPL.

Nomenclature

c: Velocity of sound in a medium at rest
D: Doppler amplification factor due to the moving source
f: A function taking into account the geometry and the kinematics of the moving surface when $f(\mathbf{x}, t) = 0$
$\mathbf{F}$: Force induced by the constant load $\rho_0 c^2$ on the moving surface
H: Heaviside function
m: Rank of harmonic
$\mathbf{M}$: Mach number associated to the absolute velocity of the source
M_r: Mach number of the sources in the direction of listening point given by $M_r = (\mathbf{r}/r) \cdot \mathbf{M}$
$\mathbf{n}$: A unit vector normal to the moving surface
p': Acoustic pressure
P': Overall acoustic pressure
$\mathbf{r}$: Distance between the observer and the source given by $\mathbf{r} = \mathbf{x} - \mathbf{y}$
s: Rank of harmonic
t: Reception time
v_n: Velocity normal to the moving surface
x: Position of the observer
y: Position of the source
α_n: Angle between two successive fan blades
δ: Dirac function
Ω: Rotational velocity in rad/s
ϕ: Observer angular position
ρ_0: Density of the propagation medium
τ: Emission time
θ: Observer angular position.

References

[1] M. P. Isom, "The theory of sound radiated by a hovering transonic helicopter blade," Poly-AE/AM 75-4, Polytechnic Institute of New York, 1975.
[2] F. Farassat, "The derivation of a thickness noise formula for the far-field by Isom," *Journal of Sound and Vibration*, vol. 64, no. 1, pp. 159–160, 1979.
[3] F. Farassat, "Extension of Isom's thickness noise formula to the near field," *Journal of Sound and Vibration*, vol. 67, no. 2, pp. 280–281, 1979.
[4] J. E. F. Williams and D. L. Hawkings, "Sound generation by turbulence and surfaces in arbitrary motion," *Philosophical Transactions for the Royal Society of London Series A*, vol. 264, no. 1151, pp. 321–342, 1969.
[5] F. Farassat, "Isom's thickness noise formula for rotating blades with finite thickness at the tip," *Journal of Sound and Vibration*, vol. 72, no. 4, pp. 550–553, 1980.
[6] G. Ghorbaniasl and C. Hirsch, "Validation and application of a far-field time domain formulation for fan noise prediction," in *Proceedings of the 11th AIAA/CEAS Aeroacoustics Conference*, pp. 497–511, March 2005.
[7] F. Farassat and C. P. Succi, "A review of propeller discrete frequency noise prediction technology with emphasis on two current methods for time domain calculations," *Journal of Sound and Vibration*, vol. 71, no. 3, pp. 399–419, 1980.
[8] S. Khelladi, S. Kouidri, and R. Rey, "Isom's thickness noise for axial and centrifugal subsonic fans," *Journal of Sound and Vibration*, vol. 313, no. 1-2, pp. 1–6, 2008.
[9] S. Khelladi, S. Kouidri, F. Bakir, and R. Rey, "Predicting tonal noise from a high rotational speed centrifugal fan," *Journal of Sound and Vibration*, vol. 313, no. 1-2, pp. 113–133, 2008.
[10] F. Farassat, "Derivation of formulations 1 and 1a of farassat," NASA-TM-2007-214853, March 2007, http://ntrs.nasa.gov.
[11] D. L. Hawkings and M. V. Lowson, "Theory of open supersonic rotor noise," *Journal of Sound and Vibration*, vol. 36, no. 1, pp. 1–20, 1974.
[12] D. Fedala, S. Kouidri, and R. Rey, "Numerical study of time domain analogy applied to noise prediction from rotating blades," *Journal of Sound and Vibration*, vol. 321, no. 3-5, pp. 662–679, 2009.
[13] S. Khelladi, S. Kouidri, F. Bakir, and R. Rey, "Flow study in the impeller-diffuser interface of a vaned centrifugal fan," *ASME Journal of Fluids Engineering*, vol. 127, no. 3, pp. 495–502, 2005.

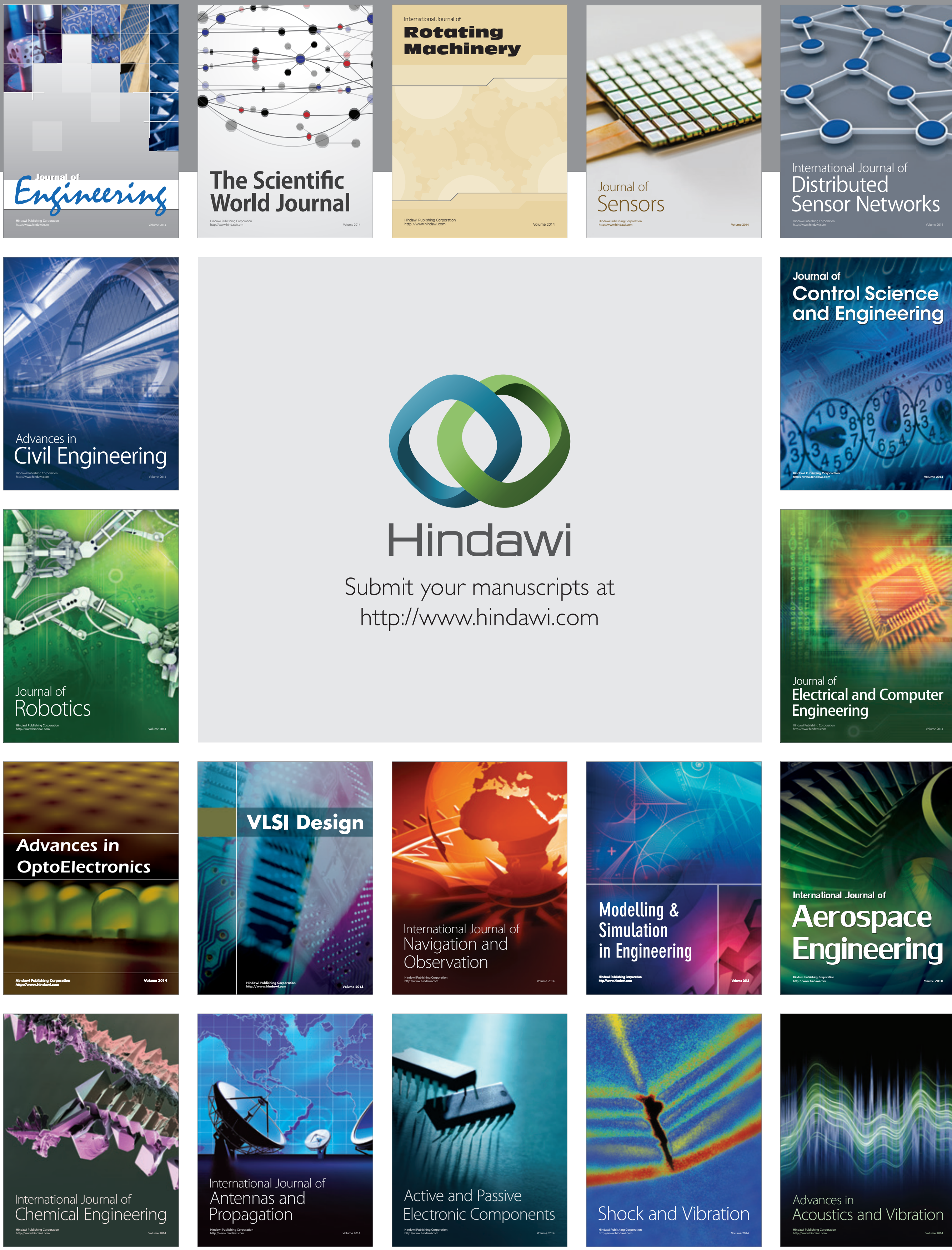
Journal of Engineering
The Scientific World Journal
International Journal of Rotating Machinery
Journal of Sensors
International Journal of Distributed Sensor Networks
Advances in Civil Engineering
Journal of Control Science and Engineering
Hindawi
Submit your manuscripts at
http://www.hindawi.com
Journal of Robotics
Journal of Electrical and Computer Engineering
Advances in OptoElectronics
VLSI Design
International Journal of Navigation and Observation
Modelling & Simulation in Engineering
International Journal of Aerospace Engineering
International Journal of Chemical Engineering
International Journal of Antennas and Propagation
Active and Passive Electronic Components
Shock and Vibration
Advances in Acoustics and Vibration